1    **Deglacial landscapes and the Late Upper Palaeolithic of Switzerland**

2

3    Hazel Reade[1*], Jennifer A. Tripp[1,7], Sophy Charlton[2,8], Sonja B. Grimm[1,3], Denise Leesch[4],

4    Werner Müller[4], Kerry L. Sayle[5], Alex Fensome[1], Thomas F.G. Higham[6], Ian Barnes[2],

5    Rhiannon E. Stevens[1]

6

7    [1] UCL Institute of Archaeology, 31-34 Gordon Square, London, WC1H 0PY, United Kingdom

8    [2] Department of Earth Sciences, Natural History Museum, Cromwell Road, London SW7

9      5BD, United Kingdom

10   [3] Centre for Baltic and Scandinavian Archaeology (ZBSA), Foundation Schleswig-Holsteinian

11     State Museums Schloss Gottorf, Schlossinsel 1, 24837 Schleswig, Germany

12   [4] Université de Neuchâtel, Laboratoire d'archéozoologie, Avenue de Bellevaux 51, CH-2000

13     Neuchâtel, Switzerland

14   [5] Scottish Universities Environmental Research Centre, Rankine Avenue, East Kilbride G75

15     0QF, United Kingdom

16   [6] Research Laboratory for Archaeology and the History of Art, University of Oxford, Dyson

17     Perrins Building, South Parks Road, Oxford OX1 3QY, United Kingdom

18

19   *corresponding author: h.reade@ucl.ac.uk, +44(0)20 7679 1530

20

21   present addresses:

22   [7] Department of Chemistry, University of San Francisco, 2130 Fulton Street, San Francisco,

23     CA 94117, USA

24   [8] PalaeoBARN, School of Archaeology, 1 South Parks Road, Oxford, OX1 3TG, United

25     Kingdom

26

**Abstract:**

The presence of people in Switzerland in recently deglaciated landscapes after the Last Glacial Maximum represents human utilisation of newly available environments. Understanding these landscapes and the resources available to the people who exploited them is key to understanding not only Late Upper Palaeolithic settlement in Switzerland, but more broadly human behavioural ecology in newly inhabited environmental settings. By applying bone collagen stable isotope analysis ($\delta^{13}C$, $\delta^{15}N$ and $\delta^{34}S$) to faunal remains from Late Upper Palaeolithic localities in Switzerland, we investigate animal ecology and environmental conditions during periods of human occupation. High and relatively uniform $\delta^{34}S$ values indicate that landscapes north of the Jura Mountains provided comparatively stable environmental conditions, while lower and more variable $\delta^{34}S$ values on the Swiss Plateau suggest a dynamic landscape with diverse hydrological and pedological conditions, potentially linked to regionally different patterns of permafrost thaw. This contrasts with the archaeological record that appears relatively uniform between the two regions, suggesting people were employing similar subsistence behaviours across a range of environmental settings. The pattern of change in $\delta^{15}N$ across the deglacial period appears consistent between areas that remained ice-free throughout the LGM and those that were glaciated. Most notable is a period of exclusively low $\delta^{15}N$ values between 15,200 and 14,800 cal. BP, which could relate a regional expansion of floral biomass in response to environmental change.

## 1. Introduction

The period after the Last Glacial Maximum (LGM) in Switzerland saw significant expansion of human settlement into previously ice-covered landscapes. This was facilitated by the rapid development of pioneer floral and faunal communities, and most likely by changes in the range dynamics of key prey species, such as horse *(Equus* sp.) and reindeer (*Rangifer tarandus*) (Leesch et al., 2012; Cupillard et al., 2015). Understanding the environmental developments that drove such changes is key to interpreting the subsistence and settlement patterns of the human populations in this region and, more broadly, to investigating human behavioural ecology in newly available landscapes. Here we examine post-LGM paleoenvironmental conditions at two archaeological localities; Kastelhöhle-Nord (Figure 1), which is situated north of the Jura Mountains and remained ice-free throughout the LGM, and Monruz and Champréveyres (Figure 1), which are situated on the Swiss Plateau and became ice-free before 17,500 cal. BP (Ivy-Ochs et al., 2004). Bone collagen stable isotope analyses ($\delta^{13}$C, $\delta^{15}$N, and $\delta^{34}$S) are applied to the archaeological faunal assemblages from these sites to provide a direct record of past prey species ecology and environmental conditions during the period of human activity. New radiocarbon dates are also obtained from the fauna to better contextualise the chronology of human occupation. By combining this data with other published results, the pattern of post-LGM environmental change is compared between regions that remained ice-free throughout the LGM and those that were glaciated.

### 1.1 Post-LGM environment and archaeology in Switzerland

Switzerland during the LGM was almost entirely covered by ice with only a small region north of the Jura Mountains remaining unglaciated (Ivy-Ochs et al., 2004; Bini et al., 2009; Ivy-Ochs 2015;). While a brief phase of human occupation during the LGM occurred in the ice-free region (Terberger and Street, 2002; Reade et al., 2020), it is not until after the LGM that evidence of widespread and sustained Late Upper Palaeolithic human activity becomes apparent (Leesch et al., 2012). Post-LGM ice sheet decay in Switzerland was rapid, and the entire central Swiss Plateau was ice free before the onset of Greenland Stadial 2.1a (GS-2.1a, c.17,450 – 14,650 BP, Figure 2; Ivy-Ochs et al., 2004; Rasmussen et al., 2014). The exposure of new landscapes during Greenland Stadial 2.1b (GS-2.1b, c. 20,850 to 17,450 BP, Figure 2; Rasmussen et al., 2014) was quickly followed by the development of pioneer floral communities. Vegetation on the northern margins of the Jura Mountains was dominated by *Poaceae*, *Artemisia*, *Juniperus* and *Hippophae* (Cupillard et al., 2015), while species-rich treeless steppe tundra had developed on the Swiss Plateau by around 18,700 cal. BP (Rey et al., 2017). This was followed by an increase in herbaceous vegetation (e.g. Ammann and Lotter, 1989; Lotter, 1999; Wehrli et al., 2007) that allowed

3

88    large herbivores to recolonise deglaciated regions by around 17,000 cal. BP (Morel and Hug,
89    1996; Hajdas et al., 2007).

90         There is some evidence for a relatively early phase of post-LGM human activity early
91    in GS-2.1a, but the main expansion of settlement in Switzerland did not occur until the latter
92    part of GS-2.1a (Weniger, 1989; Napierala, 2008; Leesch et al., 2012; Maier, 2015). These
93    sites, associated with the Magdalenian culture, are characterised by a dominance of horse
94    and reindeer in their faunal assemblages (Leesch et al., 2012; Nielsen, 2013; Maier, 2015).
95    Attributed to Magdalenian techno-complexes D and E, the sites cover a wide geographic
96    distribution across the Swiss Plateau and Jura region, indicating the exploitation of a variety
97    of landscapes (Leesch et al., 2012). Archaeological evidence comes from both caves and
98    rockshelters, such as at Kesslerloch and Kastelhöhle-Nord, and open-air localities, such as
99    the sites of Monruz and Champréveyres (Leesch et al., 2019). Coleoptera-based
100   temperature estimates suggest summer and winter mean air temperatures on the Swiss
101   Plateau during GS-2.1a were around 9°C and –20°C respectively (Coope et al., 2000; Thew
102   et al., 2009), while summer temperatures of around 12°C are estimated for the region north
103   of the Jura mountains (Cupillard et al., 2015). Pollen and plant macrofossil evidence attest to
104   vegetation rapidly increasing in diversity, but still dominated by cold-tolerant herbaceous
105   species (Thew et al., 2009; Cupillard et al., 2015).

106        The onset of Greenland Interstadial 1 (GI-1, c. 14,650 to 12,850 BP, Figure 2;
107   Rasmussen et al., 2014) corresponds to a rapid rise in temperatures on the Swiss Plateau
108   and the expansion of juniper and birch vegetation into open shrub and grasslands (Thew et
109   al., 2009). It is currently not clear whether Magdalenian activity continued into this early
110   phase of GI-1e or ended with the onset of this warm period, but by c. 14,400 cal. BP Azilian
111   occupation of the Swiss Plateau was established (Leesch et al., 2012). During this time,
112   mean summer and winter temperatures are estimated to have been around 15°C and 0°C
113   respectively, with vegetation composed of a mosaic of open birch woodland, patches of
114   dwarf birch and shrubs, and areas of grasses and sedges (Leesch, 1997; Thew et al., 2009).
115   These more temperate conditions are reflected in the change in subsistence focus, with red
116   deer (*Cervus elaphus*) and horse being important prey species (Leesch et al., 2004; Nielsen,
117   2013; Maier, 2015).

118        Considering the availability of different prey species and the ecologies and
119   environments they represent is key to understanding the landscapes past people would have
120   experienced. Whilst there is a wealth of Swiss Lateglacial palaeoenvironmental data from
121   numerous lake and mire archives (e.g. Lotter, 1999; Coope et al., 2000; Wehrli et al. 2007;
122   Lotter et al., 2012; Cupillard et al., 2015; Rey et al., 2017), analysis of the archaeological
123   faunal assemblage provides the means to directly link inferences on habitat, ecology, and
124   palaeoenvironmental conditions, to human hunting, settlement and subsistence practices.

125

### *1.2 Paleoenvironmental records from faunal stable isotopes*

126

127   Palaeoenvironmental and ecological data can be obtained directly from skeletal

128 remains of prey species from archaeological contexts through stable isotope analyses (e.g.

129 Stevens and Hedges, 2004; Stevens et al., 2008, 2014; Drucker et al., 2011a; 2011b; 2012;

130 Bocherens et al., 2015; Jones et al., 2018; Reade et al., 2020). In this study we use carbon

131 ($\delta^{13}$C), nitrogen ($\delta^{15}$N) and sulphur ($\delta^{34}$S) isotope ratios in bone collagen to explore post-

132 LGM environments and prey species ecology in Switzerland. The measured isotopic signals

133 are underpinned by dietary specialisation, animal behaviour and environmental conditions.

134   Bone collagen $\delta^{13}$C values are largely determined by species-specific dietary

135 behaviours, such as grazing versus browsing, or specific dietary specialisations, such as the

136 consumption of lichens by reindeer, which leads to systematically higher $\delta^{13}$C values in

137 comparison to other herbivore species (Drucker et al., 2010; Bocherens et al., 2015).

138 However, dietary $\delta^{13}$C values also reflect atmospheric $CO_2$ concentration and $\delta^{13}$C,

139 environmental variables such as temperature and moisture availability, and vegetation

140 density and type (Heaton, 1999; Stevens and Hedges, 2004; Drucker et al., 2008; Kohn,

141 2010). Faunal $\delta^{15}$N values are linked to both dietary specialisation/niche position and to

142 climatic parameters, such as temperature and precipitation, mediated through soil processes

143 (Amundson et al., 2003; Stevens et al., 2008; 2014; Drucker et al., 2011b; 2012; 2018

144 Craine et al 2015; Rabanus-Wallace et al., 2017). In particular, nutrient availability and

145 microbial activity may be reflected in herbivore bone collagen $\delta^{15}$N values, parameters that

146 were likely strongly influenced by the presence of permafrost and ice sheets in the European

147 Lateglacial (Stevens and Hedges, 2004; Stevens et al., 2008; Drucker et al., 2011b).

148 Collagen $\delta^{34}$S values relate to the soil environment upon which the animal fed. Bioavailable

149 sulphur can be derived from sulphates in groundwater and rain, atmospheric sulphur, and

150 from mineral weathering of the underlying geology (Nehlich, 2015). As such, bone collagen

151 $\delta^{34}$S values are spatially variable and often considered a tool for exploring mobility and

152 landscape utilisation (e.g. Drucker et al., 2012; 2018; Jones et al., 2018; Wißing et al., 2019).

153 However, bone collagen $\delta^{34}$S values may also hold significant promise as a

154 palaeoenvironmental proxy, as soil-bedrock interactions, mineral weathering, and sulphur

155 cycling in the soil are driven by hydrological and microbial processes (Thode, 1991). These

156 are dynamic systems influenced by climatic and environmental conditions, such that $\delta^{34}$S

157 values in the local landscape are unlikely to have remained static across major

158 environmental transitions, for example the last deglaciation.

159

160 **2. Materials and Methods**

161    In this study we present δ13C, δ15N and δ34S data generated from horse, reindeer,
162    red deer and *Bos/Bison* bone collagen samples from the Swiss sites of Kastelhöhle-Nord,
163    Monruz and Champréveyres to explore animal ecology and environmental conditions after
164    the LGM.

165

166    **2.1 Archaeological samples**
167    The faunal assemblage from Kastelhöhle-Nord provides a record from the ice-free
168    region of Switzerland, on the north edge of the Jura Mountains. Excavation of the cave
169    between 1948 and 1954 revealed an 'intermediate' horizon associated with a Badegoulian
170    phase of occupation, dated to the latter part of the LGM (Terberger and Street, 2002; Reade
171    et al., 2020), and a 25cm-thick 'upper' horizon associated with the post-LGM Magdalenian
172    (Leesch et al., 2012). This upper horizon contained a rich lithic assemblage that certainly
173    represents more than one phase of Magdalenian activity at the site and most likely
174    comprises more than one techno-complex (Magdalenian D-a and E; Leesch et al., 2012). A
175    relatively long duration of accumulation for this horizon was confirmed by three faunal
176    radiocarbon dates, which range from 16,350–15,965 cal. BP (ETH-45024) to 14,265–13,967
177    cal. BP (ETH-45026) (Leesch et al., 2012; Figure 2, Table 1). We sampled the large
178    herbivore species found within the upper horizon (Schweizer, 1959); reindeer (n=10), horse
179    (n=5) and *Bos/Bison* (n=6). Of these, one reindeer bone displayed evidence of
180    anthropogenic impact (cut marks). To investigate the chronology of this horizon, 3
181    specimens (two horse and the cut-marked reindeer bone) were selected for radiocarbon
182    dating. The three specimens that had previously been dated (two reindeer, one *Bos/Bison*)
183    were also re-dated to ensure methodological consistency between laboratories.
184    Comparative post-LGM samples from the Swiss Plateau, which was glaciated during
185    the LGM, come from the open-air localities of Monruz and Champréveyres. Excavated
186    between 1984 and 1992, both sites produced Late Upper Palaeolithic Magdalenian and
187    Azilian occupation horizons, with rich faunal, botanical and lithic assemblages. Phases of
188    Magdalenian activity at the sites date to the later part of GS-2.1a and were focused primarily
189    on the exploitation of horse, together with a broad spectrum of smaller mammals, birds and
190    fish, particularly in spring and summer (Müller et al., 2006; Müller, 2013). Three horse bones
191    from these assemblages have previously been radiocarbon dated, producing age
192    determinations between 15,874–15,349 cal. BP (OxA-20699) and 15,585–15,053 cal. BP
193    (OxA-20701) (Figure 2, Table 1). We selected five reindeer and 12 horse samples from
194    Monruz (all from Magdalenian sector 1) and 7 red deer samples from Champréveyres (four
195    from Magdalenian sector 2, two from Azilian sector 1, and one from sector 2 where the
196    association to the Magdalenian or Azilian was uncertain) for stable isotope analysis. While
197    the specimens do not bear direct traces of anthropogenic action, the large herbivore faunal

198 assemblage from the sites is confidently interpreted as the product of human action (Müller

199 et al., 2006; Müller, 2013). While Magdalenian activity has been dated both from faunal and

200 charcoal remains, dating of the Azilian phase has so far relied solely on charcoal samples.

201 Therefore, one bone from the Azilian concentration at Champréveyres was selected for

202 radiocarbon dating as part of this study.

203

204 **2.2 Sample pre-treatment**

205 A small sample of bone (0.2 to 1.3g) was collected from each specimen using a

206 dental drill with either a small cutting wheel or tungsten burr attachment. Samples were

207 prepared at University College London (UCL) using a modified version of the Oxford

208 Radiocarbon Accelerator Unit (ORAU) collagen extraction procedures (AF and AG methods;

209 Brock et al., 2010), which is based on a modified version of the Longin (1971) method. All

210 samples were treated with 0.5M hydrochloric acid (HCl) at 4°C until fully demineralised and

211 then thoroughly rinsed with ultrapure water. Some samples were then also treated with 0.1M

212 sodium hydroxide (30mins), and 0.5M HCl (1hr) to remove humic contaminants (Szpak et

213 al., 2017), again being thoroughly rinsed with ultrapure water between reagents. All samples

214 were then gelatinised in pH3 HCl solution at 75°C for 48hrs and filtered using a pre-cleaned

215 Ezee-filter. For most samples, including all those to be radiocarbon dated, the filtrate was

216 then passed through a pre-cleaned 15–30 kD ultrafilter, with the >30 kD fraction collected

217 and freeze-dried (AF method). For some samples the ultrafiltration step was omitted (AG

218 method); while ultrafiltration has been shown to successfully improve the removal of

219 contaminants that can influence radiocarbon determinations (Higham et al., 2006), it also

220 significantly reduces collagen yield, while at the same time producing little difference in

221 measured stable isotope compositions (Sealy et al., 2014; Szpak et al., 2017). Details of pre-

222 treatment methodology are given for each sample in the supplementary information S1.

223

224 **2.3 Stable isotope analysis**

225 Collagen yields from Kastelhöhle-Nord ranged from 2.3 to 16.2%. Collagen

226 preservation at Monruz and Champréveyres was poorer; 12 out of 24 samples failed to

227 produce enough collagen for stable isotope analysis (yields ≤0.7%), while the other 12

228 samples had collagen yields ranging from 0.8 to 3.6% (supplementary information S1).

229 Samples with adequate collagen were analysed for their nitrogen ($\delta^{15}N$), carbon ($\delta^{13}C$), and

230 sulphur ($\delta^{34}S$) isotopic ratios at the Scottish Universities Environmental Research Centre

231 (SUERC). 1.2–1.5mg aliquots of freeze-dried collagen were weighed into tin capsules and

232 analysed using a Delta V Advantage continuous-flow isotope ratio mass spectrometer

233 coupled via a ConfloIV to an EA IsoLink elemental analyser (Thermo Fisher Scientific,

234 Bremen). For every ten archaeological samples, three in-house standards, calibrated to the

7

International Atomic Energy Agency (IAEA) reference materials, were analysed (Sayle et al., 2019). Results are reported as per mil (‰) relative to the internationally accepted standards VPDB, AIR and VCDT. Measurement uncertainty was determined to be ±0.1‰ for $\delta^{13}C$, ±0.2‰ for $\delta^{15}N$, and ±0.3‰ for $\delta^{34}S$, on the basis of repeated measurements of an in-house bone collagen standard and a certified fish gelatin standard (Elemental Microanalysis, UK). Standard quality control criteria were used to assess the $\delta^{13}C$, $\delta^{15}N$ and $\delta^{34}S$ data (DeNiro, 1985; Ambrose, 1990; Nehlich and Richards, 2009). Each sample was analysed in duplicate and reproducibility was better than ±0.1‰ for $\delta^{13}C$, ±0.2‰ for $\delta^{15}N$ and ±0.3‰ for $\delta^{34}S$. All analysed samples had C:N atomic ratios between 3.2–3.6, and %C and %N between 35-46% and 12-16%, respectively, indicating good bone collagen preservation (DeNiro, 1985; Ambrose, 1990). All analysed samples except UPN-240 had C:S and N:S atomic ratios within the recommended ranges of 600 ± 300 and 200 ± 100, and %S content between 0.14 and 0.30% (Nehlich and Richards, 2009)

### 2.4 Radiocarbon analysis and background corrections

Radiocarbon dating was performed at ORAU using their standard procedures, as described by Brock *et al.* (2010). For each sample, approximately 5mg of dry collagen, which had been weighed into tin capsules baked at 500°C for 12 hours, was combusted using an elemental analyser coupled to an isotope ratio mass spectrometer, employing a splitter to allow for collection of the $CO_2$ (Bronk Ramsey and Humm, 2000; Brock at al., 2010). Samples were graphitised by reduction of collected $CO_2$ over an iron catalyst in an excess $H_2$ atmosphere at 560°C (Bronk Ramsey and Hedges, 1997; Dee et al., 2010). $^{14}C$ dates were measured on the Oxford AMS system using a cesium ion source for ionisation of the solid graphite sample (Bronk Ramsey et al., 2004). To denote the bone pretreatment at UCL rather than at ORAU, all measured dates were given "OxA-V-wwww-pp" numbers, where "wwww" indicates the wheel number, and "pp" is the position of the sample on the wheel (Brock et al., 2010). As collagen extraction was performed at UCL according to the ORAU pretreatment protocol, background corrections were applied to our dates based on repeat AMS measurements at ORAU of known-aged reference samples prepared in the UCL laboratory, following the method outlined by Wood et al. (2010). A full description of our correction methodology is detailed in Reade et al. (2020). Corrected dates are denoted by adding a "C" to the end of the date code assigned by ORAU. Uncorrected measured date values as well as further details of the correction calculations are provided in the supplemental information S2.

### 3. Results and Discussion

### 3.1 Chronology of the Lateglacial assemblage at Kastelhöhle-Nord and Champréveyres

Six new radiocarbon determinations were made on fauna from the upper horizon at Kastelhöhle-Nord (Figure 2, Table 1). Three of these were undertaken on previously dated specimens for inter-laboratory comparison, and the results reflect those previously obtained (Leesch and Müller, 2012) (Table 1). The new dates for Kastelhöhle-Nord's upper horizon range from 13,550 ± 60 ^{14}C BP (OxA-V-2794-25C) to 12,200 ± 50 ^{14}C BP (OxA-V-2793-56C), giving a range of calibrated ages between 16,350 – 15,965 cal. BP and 14,260 – 13,935 cal. BP, further confirming an extended period of bone accumulation in the horizon. There appears to be a species-based chronological pattern to the results (Figure 2); *Bos/Bison* and horse date to GS-2.1a and reindeer to GI-1. However, this finding is likely coincidental as reindeer dating to GS-2.1a are known at other sites within the same valley system (e.g. Hollenberg-Höhle 3; Müller and Leesch, 2011), as are horse dating to GI-1 (e.g. Kohlerhöhle; Leesch and Müller, 2012). Thus, both species were present within the local landscape at the same time as one another.

Archaeologically, the dating of a cut-marked reindeer bone found in association with Magdalenian artefacts to the later, colder part of GI-1ed is problematic when considered against our current understanding of the chronology of Magdalenian/Azilian development and their subsistence systems in the region. While it is recognised that the Kastelhöhle-Nord upper horizon lithic assemblage most probably represents more than one Magdalenian techno-assemblage (Leesch et al., 2012), the reindeer date is significantly later than those at other Magdalenian sites in the region and also later than dates associated with the Early Azilian assemblages at Monruz and Champréveyres. Therefore, it appears reindeer hunting at Kastelhöhle-Nord continued or resumed after the Magdalenian disappeared from the archaeological record in adjacent regions. As the bone was found in the mixed Magdalenian techno-assemblage the question arises whether this lithic tradition survived or was revived with the hunting of reindeer during GI-1ed, or whether there is a yet unrecognised lithic assemblage type admixed in the upper horizon. Comparable late GI-1ed radiocarbon dates on faunal remains (horse, ptarmigans, red deer and dog) have come from the nearby cave of Büttenloch, and from other northern Swiss localities, namely Rislisberghöhle and Kesslerloch (Napierala, 2008; Leesch and Müller, 2012). Chronologically, the dates are compatible with the Azilian phase in Switzerland, although the dated fauna cannot be certainly attributed to the subsistence activities of this culture.

One new radiocarbon determination was made on a red deer bone from the Azilian horizon at Champréveyres, which had so far been chronologically constrained by radiocarbon determinations made on charcoal and macrobotanical remains (Leesch, 1997). The date, 12,480 ± 50 ^{14}C years BP (OxA-V-2754-49C, Figure 2, Table 1), falls within the

309    range of dates on charcoal from hearth deposits, confirming the contemporaneity of the

310    faunal assemblage with human activity at the site.

311

312    ### 3.2 Lateglacial ecology and environment at Kastelhöhle-Nord and

313    ### Monruz/Champréveyres

314    Kastelhöhle-Nord upper horizon $\delta^{13}C$ values overlap for reindeer and *Bos/Bison,* (–

315    20.3‰ to –19.4‰ and –20.1‰ to –19.7‰, respectively) while horse $\delta^{13}C$ values differ (–

316    21.3‰ to –20.2‰) (Figure 3, Table 2). A similar offset between reindeer and *Bos/Bison*, and

317    horse is also observed in the nitrogen isotopic data, which ranges from 0.7‰ to 2.3‰ for

318    horse, compared to 2.3‰ to 3.5‰ and 2.6‰ to 4.0‰ for reindeer and *Bos/Bison*

319    respectively (Figure 3, Table 2). The significant species-based differences between $\delta^{13}C$ and

320    $\delta^{15}N$ values (Figure 3, supplementary information S3.1 and S3.2) can largely be explained

321    by species ecology and dietary specialisation. The comparable *Bos/Bison* and reindeer $\delta^{13}C$

322    values indicate ecological overlap. Reindeer typically display higher $\delta^{13}C$ values than other

323    herbivore species due to lichen consumption; this dietary behaviour has also been observed

324    in some modern bison populations and has previously been suggested for the species in

325    other Late Pleistocene contexts (Larter and Gates, 1991; Julien et al., 2012; Bocherens et

326    al., 2015). The two species also display similar $\delta^{15}N$ and $\delta^{34}S$ values (Figure 3, Table 2),

327    further supporting the interpretation of overlapping habitat preferences. Lower $\delta^{13}C$ and $\delta^{15}N$

328    values in horse compared to reindeer is a pattern that is observed across Pleistocene

329    Europe and indicates occupation of a different ecological niche (Stevens and Hedges, 2004;

330    Stevens et al., 2008; Bocherens et al., 2015). The $\delta^{34}S$ values observed for horse also differ

331    from those of reindeer and *Bos/Bison* (Figure 3, Table 2), further suggesting that the animals

332    were not only occupying different niches, but also possibly different landscapes and/or

333    different topographical features/locations within a given area. However, it should be noted

334    that the species-dependent chronological pattern observed in the radiocarbon dates (Figure

335    2) means that it cannot be certainly demonstrated that any of the individuals analysed here

336    overlap in their chronology, and as such, the differences observed may partly be influenced

337    by temporally changing underlying environmental parameters. Pollen records indicate the

338    vegetation north of the Jura mountains was dominated by a mosaic of *Poaceae*, *Artemisia*,

339    *Juniperus* and *Hippophae* species during GS-2.1a, with *Juniperus and Betula* expanding at

340    the start of GI-1e, while climatic proxies suggest both an increase in temperature and

341    precipitation across this time interval (Cupillard et al., 2015). Thus, the observed isotopic

342    data likely represents a combined signal of environmental change and species-specific

343    patterns of habitat utilisation.

344    A similar pattern of variation between horse and reindeer is seen in the Monruz

345    results (Figure 4). At this site average horse $\delta^{15}N$ values (1.8 ± 0.6‰) and $\delta^{13}C$ values (–

346  21.0 ± 0.2‰) are significantly different to the reindeer values (2.8 ± 0.2‰ and −19.8 ± 0.2‰,

347  respectively) (S3.3). Furthermore, $\delta^{13}$C and $\delta^{15}$N values for horse at Monruz and

348  Kastelhöhle-Nord upper horizon are indistinguishable from one another; the same is also

349  observed for reindeer from the two sites (S3.4 and S3.5). By contrast, horse and reindeer

350  $\delta^{34}$S values at Monruz are statistically indistinguishable from one another (Figure 4; S3.6),

351  but significantly different to those of the horse and reindeer at Kastelhöhle-Nord (S3.7).

352  Therefore, $\delta^{13}$C and $\delta^{15}$N values cluster by species, indicating that ecological niche and

353  animal behaviour are the primary factors influencing these values, while $\delta^{34}$S values cluster

354  by site, indicating that location-based factors are most strongly represented in the sulphur

355  isotope ratios. Almost twice as much variability is observed in the Monruz $\delta^{34}$S values

356  (16.5‰) than in the Kastelhöhle-Nord $\delta^{34}$S values (8.8‰), despite the Monruz samples

357  representing a significantly shorter time span (Figure 2) and representing only two, rather

358  than three, different animal species (Table 2). Further, unlike at Kastelhöhle-Nord, the horse

359  and reindeer $\delta^{34}$S values from Monruz completely overlap with one another. Thus, while the

360  Monruz $\delta^{13}$C and $\delta^{15}$N values suggest that horse and reindeer were occupying different

361  ecological niches, the sulphur isotopic data suggests this was likely taking place within the

362  same geographical region(s), and therefore under the same range of environmental and

363  climatic conditions. The large range in $\delta^{34}$S values could indicate both species were

364  displaying a number of different long-distance mobility behaviours, or alternatively, could

365  suggest a high level of environmental variability within a relatively small geographical region.

366  As the Monruz horse produce a significantly greater range of $\delta^{34}$S values (16.2‰) than the

367  reindeer (7.0‰), and unlike reindeer, horse generally do not undertake long-distance

368  seasonal migrations, we suggest the second interpretation is more plausible. However, we

369  recognise mobility behaviours may have differed between different environments in Late

370  Pleistocene Europe (e.g. Bignon et al., 2005; Pelligrini et al., 2008; Pryor et al., 2016).

371      The isotopic composition of bioavailable sulphur is spatially variable at a range of

372  scales. At the regional level, soil $\delta^{34}$S values are controlled by location-based inputs from

373  underlying bedrock geology, sea spray and the atmosphere (Thode, 1991; Nehlich, 2015).

374  However, Monruz and Kastelhöhle-Nord are situated far from the coast and occupy similar,

375  relatively uniform sedimentary geologies comprised of limestone, sandstone, and clay that

376  are unlikely to account for the range of $\delta^{34}$S values that we observe (Asch, 2005; Figure 1).

377  Other potential sources of spatial variation in $\delta^{34}$S values relate to more local-scale

378  differences in soil microbial activity, influenced by soil temperature, water content and

379  oxygen availability (Orchard and Cook 1983; Liu et al., 2018; Nitsch et al., 2019). Indeed,

380  paleoenvironmental records from the Swiss Plateau document a highly heterogeneous

381  landscape existed during this period; increasing temperatures led to permafrost thaw,

382  terrestrial landscape instability and the development of localised marshy habitats in some

383   areas, while in other areas it facilitated vegetation development and soil stabilisation (Thew

384   et al., 2009; Rey et al., 2017; 2019). It is these local-scale processes which we suggest are

385   represented in the high level of variation observed in the Monruz $\delta^{34}S$ values.

386          Only one result is available for the Azilian period from Monruz and Champréveyres.

387   This was the sole sample from an Azilian context at Champréveyres to yield adequate

388   collagen for analysis, and the only red deer sample in our data set. This sample produced

389   $\delta^{13}C$ and $\delta^{15}N$ values of –20.6‰ and 2.4‰, respectively, which are comparable to the red

390   deer previously analysed from the site (–20.6‰ and 3.4‰, Drucker et al., 2009).

391

### Deglaciated versus unglaciated Lateglacial landscape development

393          In the context of Late Pleistocene Europe, much of the spatial and temporal variation

394   observed in herbivore bone collagen stable isotope values has been linked to soil processes,

395   related to variations in temperature, permafrost extent and proximity to ice sheet margins

396   (Stevens and Hedges, 2004; Stevens et al., 2008; Drucker et al., 2011b; 2012). To explore

397   these possible drivers of the isotopic signatures, and by inference post-LGM environmental

398   change, we compare the temporal patterns observed in fauna from neighbouring regions

399   that had been glaciated at the LGM to those that had remained ice-free during the last

400   glacial cycle. We combine the results of this study with those previously published from

401   regions of Switzerland, the French Jura and Western Alps (Drucker et al., 2003; 2009;

402   2011a; 2011b; 2012; Stevens et al., 2008; Bocherens et al., 2011; Gröcke et al., 2017;

403   Reade et al., 2020; Figure 5; Supplementary Information 5). Sites are assigned to two

404   groups based on reconstructed maximum ice extents; those in locations that remained ice-

405   free through the LGM, and those that were ice-covered at the LGM (Campy, 1992; Bini et al.,

406   2009; Schlüchter et al., 2010). As this analysis combines data from multiple species

407   (*Bos/Bison*, horse, red deer, and reindeer), differences in dietary behaviours mask possible

408   environmental interpretations from the $\delta^{13}C$ values. Dietary ecology is also likely responsible

409   for some of the scatter in the $\delta^{15}N$ data, but temporal trends are nonetheless apparent

410   (Figure 5). Herbivore $\delta^{34}S$ values appear to primarily reflect the underlying environment,

411   irrespective of differences in dietary ecology, and the different temporal patterns in the $\delta^{34}S$

412   values between the two location-based groups is striking (Figure 5).

413          For $\delta^{15}N$ values, the temporal pattern of variation appears consistent between the

414   ice-covered and ice-free areas, suggesting that the presence/absence of ice sheets and

415   processes of deglaciation are not the direct primary influences being recorded in the signal.

416   The most notable aspect of the record is the absence of $\delta^{15}N$ values greater than c. 2.5‰

417   between around 15,200 and 14,800 cal. BP. As this pattern is present in samples that span

418   a large geographical area, which is topographically and environmentally diverse, a regional-

419   scale explanation should be sought. Low herbivore $\delta^{15}N$ values (<2.5‰ ) in Lateglacial

420  Europe have previously been linked to environments with nutrient-poor soils, where low
421  temperatures and the presence of permafrost impeded the soil nitrogen cycle, or to
422  increased environmental moisture; conversely, high herbivore $\delta^{15}N$ values (>5‰) have been
423  considered typical of environments where nitrogen supply is not a limiting factor to plant
424  growth and environmental conditions do not inhibit the soil nutrient cycle (Schulze et al.,
425  1994; Hobbie et al., 1998; Jonasson et al., 1999; Stevens and Hedges 2004; Stark, 2007;
426  Stevens et al., 2008; 2009; Drucker et al., 2011b; 2012; Rabanus-Wallace et al., 2017). Low
427  $\delta^{15}N$ values occur alongside an absence of high $\delta^{15}N$ values at various points in the
428  Swiss/French record shown in Figure 5 (at c. 21,000 – 18,200 cal. BP, c. 15,200 – 14,800
429  cal. BP, and c. 12,200 cal. BP). However, we suggest that it is only the 15,200 – 14,800 cal.
430  BP interval that can be discussed with a degree of confidence, as the exclusively low $\delta^{15}N$
431  values during this time interval are clearly bounded by the presence of higher $\delta^{15}N$ values
432  both before and after (Figure 5). The timing of this disappearance of $\delta^{15}N$ values greater
433  than c. 2.5‰ in the Swiss/French record broadly corresponds to the end of Heinrich Event 1
434  (HE1), a period of climatic cooling following the LGM, during which Alpine ice sheets
435  expanded (Hemming, 2004; Ivy-Ochs et al., 2006). Immediately after HE1, a small but
436  significant climatic warming is evident, although lake level data suggests annual precipitation
437  amounts remained relatively low (Magny et al., 2006; Magny, 2013). On the Swiss Plateau
438  localised permafrost degradation and an increase in insect and plant species diversity is
439  evident (Thew et al., 2009; Rey et al., 2017). A similar increase in vegetation density is also
440  evident northwest of the Jura mountains (e.g. Magny et al., 2006). It is possible that if this
441  period corresponds to the first significant regional increase in vegetation after the LGM, such
442  an increase even if relatively small, occurring in an already nutrient-limited environment
443  would initially deplete nutrient availability even further. The effect of this would be a short-
444  term decline in average plant $\delta^{15}N$ values, followed by a rapid increase, as soils matured and
445  nutrient cycling accelerated (Hobbie et al., 1998; 2005; Ammann et al., 2013).

446       Unlike the nitrogen record, sulphur isotope ratios display a significantly different
447  pattern of change between ice-covered and ice-free areas. Ice-free areas display low $\delta^{34}S$
448  values (<–8‰) at around 23,000 cal. BP, but then remain consistently high across the
449  deglacial period (>–8‰, except for one outlier). By contrast, in locations that were covered
450  by ice at the LGM, low $\delta^{34}S$ values (<–8‰) are recorded at around 15,900 to 15,400 cal. BP,
451  increasing to a minimum of –5‰ by 15,000 cal. BP. While some of the scatter in the data
452  can be explained by different patterns of mobility between different species, such influences
453  cannot explain the clear location-specific differences in the temporal sulphur isotopic record.
454  Further, while location-based geological differences may produce different absolute $\delta^{34}S$
455  values, no relationship is observed between bedrock type, $\delta^{34}S$, and glaciated/ ice-free
456  location (Figure S4). As such, spatially and temporally variable environmental parameters

13

457 need to be considered. Temperature-mediated controls on soil mineralisation and
458 volatilisation, and bacterial reduction of sulphur have been suggested to explain temporal
459 changes in herbivore $\delta^{34}$S values (Drucker et al., 2011a). However, temperature change
460 alone cannot explain the location-based differences we observe in the data, unless it was
461 acting on a sub-regional scale. Soil maturity has also been linked to differences in herbivore
462 sulphur isotopic ratios (Drucker et al., 2012), but this interpretation is not supported in this
463 instance by the corresponding $\delta^{15}$N values.

464      Here, we suggest that the herbivore $\delta^{34}$S values reflect local soil conditions that are
465 primarily related to hydrology and microbial activity. Plants acquire sulphur from the soil as
466 sulphate, derived from mineral weathering and atmospheric deposition, and influenced by
467 soil microbial action (Walker, 1957; Krouse, 1980; Robinson and Bottrell, 1997; Newton and
468 Bottrell, 2007). Changing soil hydrological dynamics, particularly the development of water-
469 logged environments that result in anaerobic conditions, can lead to significant differences in
470 plant $\delta^{34}$S values brought about by changing bacteria-mediated fractionations (Fry et al.,
471 1982; Trust and Fry, 1992; Groscheová et al., 2000; Nitsch et al., 2019). While the
472 processes that govern soil $\delta^{34}$S in relation to changing hydrological conditions are complex
473 and not yet fully understood (Mandernack et al., 2000; Nitsch et al., 2019), we suggest that
474 the different pattern observed between the ice-free and recently-deglaciated regions in post-
475 LGM Switzerland could relate to location specific hydrological dynamics, potentially related
476 ice sheet melt, or more likely, permafrost thaw processes. Indeed, the palaeoenvironmental
477 record from Lake Neuchâtel on the Swiss Plateau identifies a period of permafrost thaw
478 coinciding with considerable instability of the terrestrial landscape and localised marshy
479 conditions, that is largely contemporaneous with the low herbivore $\delta^{34}$S values identified in
480 this study at Monruz (Thew et al., 2009). By contrast, while there is greater debate about the
481 distribution and character of permafrost north and west of the Jura, recent studies suggest
482 that if present, it did not persist into the latter part of GS-2.1a (Renssen and Vandenberghe,
483 2003; Bertran et al., 2014; Vandenberghe et al., 2014). This could explain why low $\delta^{34}$S
484 values during GS-2.1a are not observed in these regions.
485
486 **Conclusion**
487
488      The carbon, nitrogen and sulphur isotopic ratios reported in this study attest to
489 regionally variable environmental development in post-LGM Switzerland. Significant
490 differences between areas that remained ice-free throughout the last glacial cycle and those
491 that were glaciated at the LGM are identified. Deriving such information from archaeological
492 faunal assemblages allows these environmental records to be directly related to human
493 presence in these areas, and to subsistence and settlement strategies in such landscapes,

14

which can more broadly inform on human behavioural ecology in peripheral settings. Our results show the post-LGM period in Switzerland and adjacent regions was characterised by diverse environmental conditions, indicating that a range of habitats and landscapes were available for humans and animals to exploit. Herbivore $\delta^{13}C$ and $\delta^{15}N$ values are most strongly influenced by species ecology and dietary behaviours, underpinned by environmental influences. $\delta^{34}S$ values appear to most strongly correspond to location-specific environmental conditions. Our results suggest that during the period of Magdalenian activity in Switzerland the Swiss Plateau was a dynamic and diverse landscape, while greater environmental stability may have existed north of the Jura Mountains.

The absence of high (>2.5‰) $\delta^{15}N$ values between 15,200 and 14,800 cal. BP, both on the Swiss Plateau and north of the Jura, indicates a regional-scale environmental phenomenon that we suggest is related to the combination of prolonged low temperatures, limited bioavailable soil nutrients, and elevated nutrient demand from increasing vegetation cover. In contrast, low (<–8‰) $\delta^{34}S$ values occur at different times in different locations, and we suggest that these reflect locally variable hydrological dynamics, either related to changing rates of mineral weathering and soil-bedrock interactions or to changing soil redox conditions, which govern microorganism-mediated isotopic fractionations. We suggest that either interpretation is congruous with the regionally different patterns of ice sheet melt and permafrost thaw.

**Author contributions**

Conceptualization: RES, HR, SG, TH & IB; Sample collection: HR, SC, DL, WM; Formal analysis: HR, JT, AF, & KLS; Investigation: HR, JT & RES; Supervision: RES; Writing - original draft: HR; Writing - review & editing: all authors; Funding acquisition: RES.

**Reference:**

Ambrose SH (1990) Preparation and characterization of bone and tooth collagen for isotopic analysis. J Archaeol Sci 17(4):431-451. https://doi.org/10.1016/0305-4403(90)90007-R

530     Ammann B, Lotter AF (1989) Late-Glacial radiocarbon- and palynostratigraphy on the Swiss
531          Plateau. Boreas 18:109-126. https://doi.org/10.1111/j.1502-3885.1989.tb00381.x

532     Ammann B, van Leeuwn JFN, van der Knapp WO, Lischke H, Heiri O, Tinner W. (2013)
533          Vegetation responses to rapid warming and to minor climatic fluctuations during the
534          Late-Glacial Interstadial (GI-1) at Gerzensee (Switzerland). Palaeogeogr Palaeocl
535          391:40-59. https://doi.org/10.1016/j.palaeo.2012.07.010.

536     Amundson R, Austin AT, Schuur EAG, Yoo K, Matzek V, Kendall C, Uebersax A, Brenner D,
537          Baisden WT (2003) Global patterns of the isotopic composition of soil and plant
538          nitrogen. Global Biogeochem Cy 17(1): 1031. https://doi.org/10.1029/2002GB001903

539     Asch K. (2005) IGME 5000: 1:5 Million International Geological Map of Europe and Adjacent
540          Areas. BGR (Hannover).

541     Bertran P, Andrieux E, Antoine P, Coutard S, Deschodt L, Gardère P, Hernandez M, Legentil
542          C, Lenoble A, Liard M, Mercier N, Moine O, Sitzia  L, Van Vliet-Lanoë B (2014)
543          Distribution and chronology of Pleistocene permafrost features in France: database
544          and first results. Boreas 43:699-711. https://doi.org/10.1111/bor.12025

545     Bignon O, Baylac M, Vigne J-D, Eisenmann V (2005) Geometric morphometrics and the
546          population diversity of Late Glacial horses in Western Europe (*Equua caballus*
547          *arcelini*): phylogeographic and anthropological implications. J Archaeol Sci 32(2):375-
548          391. https://doi.org/10.1016/j.jas.2004.02.016

549     Bini A, Buoncristiani J-F, Couterrand S, Ellwanger D, Fleber M, Florineth D, Graf HR, Keller
550          O, Kelly M, Schlüchter C, Schoeneich P (2009) La Suisse durant le denier maximum
551          glaciaire (LGM) 1:500000. Federal Office of Topography Swisstopo, Switzerland.

552     Bocherens H, Drucker DG, Taubald H (2011) Preservation of bone collagen sulphur isotopic
553          compositions in an early Holocene river-bank archaeological site. Palaeogeogr
554          Palaeocl 310(1-2):32-38. https://doi.org/10.1016/j.palaeo.2011.05.016

555     Bocherens H, Drucker DG, Germonpré M, Lázničková M, Naito WI, Wissing C, Brůžek J,
556          Oliva M (2015) Reconstruction of the Gravettian food-web at Předmostí I using multi-
557          isotopic tracking ($^{13}$C, $^{15}$N, $^{34}$S) of bone collagen. Quatern Int 359-360:211-228.
558          https://doi.org/10.1016/j.quaint.2014.09.044

559     Brock F, Higham TFG, Ditchfield P, Bronk Ramsey C (2010) Current pretreatment methods
560          for AMS radiocarbon dating at the Oxford Radiocarbon Accelerator Unit (ORAU)
561          Radiocarbon 52:103-112. https://doi.org/10.1017/S0033822200045069.

562     Bronk Ramsey C, Higham T, Leach P (2004) Towards High-Precision AMS: Progress and
563          Limitations. Radiocarbon 46(1): 17-24. https://doi.org/10.1017/S0033822200039308

564     Campy M (1992) Palaeogeographical relationships between Alpine and Jura glaciers during
565          the two last Pleistocene glaciations. Palaeogeogr Palaeocl 93(1-2):1-12.
566          https://doi.org/10.1016/0031-0182(92)90180-D

567    Coope GR, Elias SA (2000) The environment of Upper Palaeolithic (Magdalenian and

568        Azilian) hunters at Hauterive-Champréveyres, Neuchâtel, Switzerland, interpreted

569        from coleopteran remains. J Quaternary Sci 15:157–175.

570        https://doi.org/10.1002/(SICI)1099-1417(200002)15:2<157::AID-JQS478>3.0.CO;2-K

571    Craine JM, Elmore AJ, Wang L, Augusto L, Baisden WT, Brookshire ENJ, Cramer MD,

572        Hasselquist NJ, Hobbie EA, Kahmen A, Koba K, Kranabetter JM, Mack MC, Marin-

573        Spiotta E, Mayor JR, McLauchlan KK, Michelsen A, Nardoto GB, Oliveira RS, Perakis

574        SS, Peri PL, Quesada CA, Richter A, Schipper LA, Stevenson BA, Turner BL, Viani

575        RAG, Wanek W, Zeller B (2015) Convergence of soil nitrogen isotopes across global

576        climate gradients. Sci Report 5:8280. https://doi.org/10.1038/srep08280

577    Cupillard C, Magny M, Bocherens H, Bridault A, Bégeot C, Bichet V, Bossuet G, Drucker

578        DG, Gauthier E, Jouannic G, Millet L, Richard H, Ruis D, Ruffaldi P, Walter-Simonnet

579        A-V (2015)  Changes in ecosystems, climate and societies in the Jura Mountains

580        between 40 and 8 ka cal BP. Quaternary Int 378:40-72.

581        https://doi.org/10.1016/j.quaint.2014.05.032.

582    DeNiro MJ (1985) Postmortem preservation and alteration of in vivo bone collagen isotope

583        ratios in relation to palaeodietary reconstruction. Nature 317:806-809.

584        https://doi.org/10.1038/317806a0.

585    Drucker DG, Bocherens H, Bridault A, Billiou D (2003) Carbon and nitrogen isotopic

586        composition of red deer (Cervus elaphus) collagen as a tool for tracking

587        palaeoenvironmental change during the Late-Glacial and Early Holocene in the

588        northern Jura (France). Palaeogeog Palaeocl 195:375-388.

589        https://doi.org/10.1016/S0031-0182(03)00366-3.

590    Drucker DG, Bridault A, Hobson KA, Szuma E, Bocherens H (2008) Can carbon-13 in large

591        herbivores reflect the canopy effect in temperate and boreal ecosystems? Evidence

592        from modern and ancient ungulates. Palaeogeogr Palaeocl 266:69–82.

593        https://doi.org/10.1016/j.palaeo.2008.03.020.

594    Drucker DG, Bocherens H, Billiou D (2009) Quelle valence écologique pour les rennes et

595        autres cervidés au Tardiglaciaire dans les Alpes du nord et le Jura? Résultats de

596        l'analyse des isotopes stables ($^{13}$C, $^{15}$N) du collagène, in: Pion G (Ed), La fin du

597        Paléolithique supérieur dans les Alpes du nord françaises et le Jura méridional, vol.

598        50, Mémoire de la Société préhistorique française, Paris, pp 73-86.

599    Drucker DG, Bridault A, Cupillard C,  Hujic A, Bocherens H (2011a) Evolution of habitat and

600        environment of red deer *(Cervus elaphus)* during the Late-glacial and early Holocene

601        in eastern France (French Jura and the western Alps) using multi-isotope analysis

602        ($\delta^{13}$C, $\delta^{15}$N, $\delta^{18}$O, $\delta^{34}$S) of archaeological remains. Quatern Int 245:268-278.

603        https://doi.org/10.1080/10256010903388410.

604 Drucker DG, Kind CJ, Stephan E (2011b) Chronological and ecological information on Late-
605    glacial and early Holocene reindeer from northwest Europe using radiocarbon (14C)
606    and stable isotope ($^{13}$C, $^{15}$N) analysis of bone collagen: case study in southwestern
607    Germany. Quatern Int 245(2):218-224. https://doi.org/10.1016/j.quaint.2011.05.007.

608 Drucker DG, Bridault A, Cupillard, C (2012) Environmental context of the Magdalenian
609    settlement in the Jura Mountains using stable isotope tracking ($^{13}$C, $^{15}$N, $^{34}$S) of bone
610    collagen from reindeer *(Rangifer tarandus).* Quatern Int 272-273:268-278.
611    https://doi.org/10.1016/j.quaint.2012.05.040.

612 Drucker DG, Stevens RE, Germonpré M, Sablin MV, Bocherens H (2018) Collagen stable
613    isotopes provide insights into the end of the mammoth steppe in the central East
614    European plains during the Epigravettian. Quaternary Res 90:457-469.
615    https://doi.org/10.1017/qua.2018.40.

616 Fry B, Scalan RS, Winters JK, Parker PL, (1982) Sulphur uptake by salt grasses,
617    mangroves, and seagrasses in anaerobic sediments. Geochim Cosmochim Ac
618    46:1121–1124. https://doi.org/10.1016/0016-7037(82)90063-1.

619 Gröcke DR, Sauer PE, Bridault A, Drucker DG, Germonpré M, Bocherens H (2017)
620    Hydrogen isotopes in Quaternary mammal collagen from Europe. J Archaeol Sci Rep
621    11:12-16. https://doi.org/10.1016/j.jasrep.2016.11.020

622 Groscheová H, Novák M, Alewell C (2000) Changes in the δ$^{34}$S ratio of pore-water sulfate in
623    incubated Sphagnum peat. Wetlands 20:62–69. https://doi.org/10.1672/0277-
624    5212(2000)020[0062:CITSRO]2.0.CO;2

625 Hajdas I, Bonani G, Furrer H, Mäder A, Schoch W (2007) Radiocarbon chronology of the
626    mammoth site at Niederweningen, Switzerland: results from dating bones, teeth, wood
627    and peat. Quatern Int 164-165:98-105. https://doi.org/10.1016/j.quaint.2006.10.007.

628 Heaton THE (1999) Spatial, Species, and Temporal Variations in the$^{13}$C/$^{12}$C Ratios of C$_3$
629    Plants: Implications for Palaeodiet Studies. J Archaeol Sci 26(6):637-649.
630    https://doi.org/10.1006/jasc.1998.0381

631 Hedges, REM, Stevens, RE, Kock PL (2005) Isotopes in bones, in: Leng MJ (Ed), Isotopes
632    in palaeoenvironmental research, vol. 10, Developments in palaeoenvironmental
633    research, Dordrecht, pp 117-145.

634 Hemming S. 2004. Heinrich events: massive late Pleistocene detritus layers of the North
635    Atlantic and their global climate imprint. Reviews of Geophysics 42: 1–43.

636 Higham TG, Jacobi RM, Bronk Ramsey C (2006) AMS radiocarbon dating of ancient bone
637    using ultrafiltration. Radiocarbon 48(2):179-195.
638    https://doi.org/10.1017/S0033822200066388.

639 Hobbie E, Macko SA, Shugart HH (1998) Patterns of N dynamics and N isotopes during
640     primary succession in Glacier Bay, Alaska. Cheml Geol 152:3-11.
641     https://doi.org/10.1016/S0009-2541(98)00092-8.
642 Hobbie EA, Jumpponen A, Trappe J (2005) Foliar and fungal 15N:14N ratios reflect
643     development of mycorrhizae and nitrogen supply during primary succession: testing
644     analytical models. Oecologia 146:258-268. https://doi.org/10.1007/s00442-005-0208-
645     z.
646 Ivy-Ochs S (2015) Glacier variations in the European Alps at the end of the last glaciation.
647     Cuadernos de Investigación Geográfica 41(2):295-315.
648     https://doi.org/10.18172/cig.2750.
649 Ivy-Ochs, S, Kerschner H, Kubik, PW, Schlüchter C. (2006) Glacier response in the
650     European Alps to Heinrich Event 1 cooling: the Gschnitz stadial. J. Quaternary Sci 21:
651     115–130. ISSN 0267-8179.
652 Ivy-Ochs, S, Schäfer J, Kubik PW, Synal H-A, Schlüchter C (2004) The timing of
653     deglaciation on the northern Alpine foreland (Switzerland). Eclogae Geol Helv 97:47-
654     55. https://doi.org/10.1007/s00015-004-1110-0.
655 Jonasson S, Michelsen A, Schmidt IK (1999) Coupling of nutrient cycling and carbon
656     dynamics in the Arctic; integration of soil microbial and plant processes. Appl. Soil
657     Ecol 11:135– 146. https://doi.org/10.1016/S0929-1393(98)00145-0.
658 Jones JR, Richards MP, Reade H, de Quiros FB, Marin-Arroyo AB (2018) Multi-Isotope
659     investigations of ungulate bones and teeth from El Castillo and Covalejos caves
660     (Cantabria, Spain): Implications for paleoenvironment reconstructions across the
661     Middle-Upper Palaeolithic transition. J Archaeol Sci Rep 23:1029-1042.
662     https://doi.org/10.1016/j.jasrep.2018.04.014
663 Julien M-A, Bocherens H, Burke A, Drucker DG, Patou-Mathis M, Krotova O, Péan S (2012)
664     Were European steppe bison migratory? $^{18}$O, $^{13}$C and Sr intra-tooth isotopic variations
665     applied to a palaeoethological reconstruction. Quaternary Int, 271:106-119.
666     https://doi.org/10.1016/j.quaint.2012.06.011.
667 Kohn MJ (2010) Carbon isotope compositions of terrestrial C3 plants as indicators of
668     (paleo)ecology and (paleo)climate. P Natl Acad Sci USA 107(46):19691-19695.
669     https://doi.org/10.1073/pnas.1004933107
670 Krouse HR (1980) Sulfur isotopes in our environment, in: Fritz P, Fontes JC (Eds),
671     Handbook of Environmental Isotope Geochemistry, Amsterdam, pp.435–471.
672 Larter NC, Gates CC (1991) Diet and habitat selection of wood bison in relation to seasonal
673     changes in forage quantity and quality. Can Jo Zool 69:2677–2685
674     https://doi.org/10.1139/z91-376.

Leesch, D (1997) Hauterive-Champréveyres. Un campement magdalénien au bord du lac de Neuchâtel. Cadre chronologique et culturel, mobilier et structures, analyse spatiale (secteur 1). Archéologie neuchâteloise, 19, Office et musée cantonal d'archéologie, Neuchâtel.

Leesch D, Müller W (2012) Neue Radiokarbondaten an Knochen, Zähnen und Geweih aus Magdalénien-Fundstellen der Schweiz und ihre Bedeutung für die Stellung des Magdalénien innerhalb des Spätglazials. Jahrbuch der Archäologie Schweiz 95:117–126. https://doi.org/10.5169/seals-392487.

Leesch D, Cattin, M-I, Müller W (2004) Témoins d'implantations magdaléniennes et aziliennes sur la rive nord du lac de Neuchâtel. Archéologie neuchâteloise, 31, Office et musée cantonal d'archéologie, Neuchâtel.

Leesch D, Müller W, Nielsen E, Bullinger J (2012) The Magdalenian in Switzerland: Re-colonization of a newly accessible landscape. Quatern Int 272-273:191-208 doi:10.1016/j.quaint.2012.04.010.

Leesch D, Bullinger J, Müller W (2019) Vivre en Suisse il y a 15000 ans. Le Magdalénien. Bâle, Archéologie suisse.

Longin R (1971) New method of collagen extraction for radiocarbon dating. Nature 230(5291):241–2. https://doi.org/10.1038/230241a0

Lotter AF (1999) Late-glacial and Holocene vegetation history and dynamics as shown by pollen and plant macrofossil analyses in annually laminated sediments from Soppensee, central Switzerland. Veget Hist Archaeobot 8: 165-184. https://doi.org/10.1007/BF02342718.

Lotter AF, Heiri O, Brooks S, van Leeuwen JFN, Eicher U, Ammann B (2012) Rapid summer temperature changes during Termination 1a: high-resolution multi-proxy climate reconstructions from Gerzensee (Switzerland). Quaternary Sci Rev 36:103-113. https://doi.org/10.1016/j.quascirev.2010.06.022.

Liu Y, He N, Wen X, Xu L, Sun X, Yu G, Liang L, Schipper LA (2018) The optimum temperature of soil microbial respiration: patterns and controls. Soil Biol Biochem 121:35-42.

Magny M (2013) Climatic and environmental changes reflected by lake-level fluctuations at Gerzensee from 14,850 to 13,050 yr BP. Palaeogeogr Palaeocl 391:33-39. https://doi.org/10.1016/j.palaeo.2012.05.003

Magny M, Aalbersberg G, Bégeot C, Benoit-Ruffaldi P, Bossuet G, Disnar JR, Heiri O, Laggoun-Defarge F, Mazier F, Millet L, Peyron O, Vannière B, Walter-Simmonnet AV (2006) Environmental and climatic changes in the Jura mountains (eastern France) during the Lateglacial-Holocene transition: a multiproxy record from Lake Lautrey. Quaternary Sci Rev 25:414-445. https://doi.org/10.1016/j.quascirev.2005.02.005.

712 Maier A (2015) The Central European Magdalenian: Regional Diversity and Internal
713     Variability, Springer Netherlands, Dordrecht.

714 Mandernack KW, Lynch L, Krouse HR, Morgan MD (2000) Sulfur cycling in wetland peat of
715     the New Jersey pinelands and its effect on stream water chemistry. Geochim
716     Cosmochim Ac 64:3949–64. https://doi.org/10.1016/S0016-7037(00)00491-9.

717 Morel P, Hug B, (1996) Découverte d'un crâne tardiglaciaire de rhinocéros laineux
718     *Coelodonta antiquitatis* (Blumenbach 1799) dans le lac de Neuchâtel, au large de
719     Vaumarcus (NE). Paléontologie et conservation. Bulletin de la Société neuchâteloise
720     des Sciences naturelles 119:101-110.

721 Müller W (2013) Le site magdalénian de Monruz, 3. Acquisition, traitement et consommation
722     des ressources animales. Archéologie neuchâteloise, 49, Office et musée cantonal
723     d'archéologie, Neuchâtel.

724 Müller W, Leesch D (2011) Einige Neubestimmungen aus der Magdalénien-Fundstelle
725     Hollenberg-Höhle 3 bei Arlesheim (Basel-Landschaft) und daraus folgende
726     Überlegungen zur Nutzung der Höhle. Jahrbuch der Archäologie Schweiz 94:7–20.
727     https://doi.org/ 10.5169/seals-179208.

728 Müller W, Leesch D, Bullinger J, Cattin M-I, Plumettaz N (2006) Chasse, habitats et rythme
729     des déplacements: réflexions à partir des campements magdaléniens de
730     Champréveyres et Monruz (Neuchâtel, Suisse). Bull Soc préhist fr 103(4):741-752.

731 Napierala H (2008) Die Tierknochen aus dem Kesslerloch. Neubearbeitung der
732     paläolitischen Fauna. Beiträge zur Schaffhauser Archäologie 2. Baudepartement des
733     Kantons Schaffhausen, Kantonsarchäologie, Schaffhausen.

734 Nehlich O (2015) The application of sulphur isotope analyses in archaeological research: A
735     review. Earth-Sci Rev 142:1-17. https://doi.org/10.1016/j.earscirev.2014.12.002.

736 Nehlich O, Richards MP (2009) Establishing quality criteria for sulphur isotope analysis of
737     archaeological bone collagen. Archaeol Anthrop Sci 1:59–75.
738     https://doi.org/10.1007/s12520-009-0003-6

739 Newton R, Bottrell S (2007) Stable isotopes of carbon and sulphur as indicators of environmental
740     change: past and present. J Geol Soc 164:691-708, https://doi.org/10.1144/0016-
741     76492006-101.

742 Nielsen EH (2013) Response of the Lateglacial fauna to climatic change. Palaeogeogr
743     Palaeocl 391:99-110.https://doi.org/10.1016/j.palaeo.2012.12.012

744 Nitsch EK, Lamb AL, Heaton THE, Vaiglova P, Fraser R, Hartman G, Moreno-Jiménex,
745     López-Piñeiro A, Peña-Abades D, Fairbairn A, Eriksen J, Bogaard A (2019) The
746     Preservation and Interpretation of $\delta^{34}$S Values in Charred Archaeobotanical Remains.
747     Archaeometry 61(1):161-178. https://doi.org/10.1111/arcm.12388.

748 Orchard VA, Cook FJ (1983). Relationship between soil respiration and soil moisture. Soil
749     Biol Biochem 15(4):447-453.
750 Pelligrini M, Donahue RE, Chenery C, Exans J, Lee-Thorp J, Montgomery J, Mussi M (2008)
751     Faunal migration in late-glacial central Italy: implications for human resource
752     exploitation. Rapid Commun Mass Sp 22(11):1714-1726.
753     https://doi.org/10.1002/rcm.3521
754 Pryor AJ, Stevens RE, Pike AWG (2016) Seasonal mobility of the adult horse killed by
755     hunters at Klementowice. In: Wisniewski, T (ed) Klementowice. A Magdalenian site in
756     Eastern Poland. Lublin, PL, Instytut Archeologii Uniwersytetu Marie Curie Sklodowskiej
757     pp. 298-304.
758 Rabanus-Wallace M, Wooller M, Zazula G, Shute E, Jahren AH, Kosintsev P, Burns JA,
759     Breen J, Llamas B, Cooper A (2017) Megafaunal isotopes reveal role of increased
760     moisture on rangeland during late Pleistocene extinctions. Nat Ecol Evol 1:0125.
761     https://doi.org/10.1038/s41559-017-0125
762 Rasmussen SO, Bigler M, Blockley SP, Blunier T, Buchardt SL, Clausen HB, Cvijanovic I,
763     Dahl-Jensen D, Johnsen SJ, Fischer H, Gkins V, Guillevic M, Hoek WZ, Lowe JJ,
764     Pedro JB, Popp T, Seierstad IK, Steffensen JP, Svensson AM, Vallelonga P, Vinther
765     BM, Walker MJC, Wheatley JJ, Winstrup M (2014) A stratigraphic framework for
766     abrupt climatic changes during the Last Glacial period based on three synchronized
767     Greenland ice-core records: refining and extending the INTIMATE event stratigraphy.
768     Quaternary Sci Rev 106:14-28 https://doi.org/10.1016/j.quascirev.2014.09.007.
769 Reade H, Tripp JA, Charlton S, Grimm SB, Sayle KL, Fensome A, Higham TFG, Barnes I,
770     Stevens RES (2020) Radiocarbon chronology and environmental context of Last
771     Glacial Maximum human occupation in Switzerland. Sci Rep **10:**4694
772     https://doi.org/10.1038/s41598-020-61448-7
773 Renssen, H, Vandenberghe J (2003) Investigation of the relationship between permafrost
774     distribution in NW Europe and extensive winter sea-ice cover in the North Atlantic
775     Ocean during the cold phases of the Last Glaciation. Quaternary Sci Rev 22:209–223.
776     https://doi.org/10.1016/S0277-3791(02)00190-7
777 Rey F, Gobet E, van Leeuwen JFN, Gilli A, van Raden UJ, Hafner A, Wey O, Rhiner J,
778     Schmocker D, Zünd J, Tinner W (2017) Vegetational and agricultural dynamics at
779     Burgäschisee (Swiss Plateau) recorded for 18,700 years by multi-proxy evidence
780     from partly varved sediments. Veg Hist Archaeobot 26(6):571-586.
781     https://doi.org/10.1007/s00334-017-0635-x
782 Rey F, Gobet E, Schwörer C. Hafner A, Tinner W (2019, in review) Climate impacts on
783     deglaciation and vegetation dynamics since the Last Glacial Maximum at Moossee
784     (Switzerland). Clim Past Discuss. https://doi.org/10.5194/cp-2019-121

785 Robinson BW, Bottrell SH (1997) Discrimination of sulphate sources in pristine and polluted
786     New Zealand river catchments using stable isotopes. Appl. Geochem. 12: 305–319.
787     https://doi.org/10.1016/S0883-2927(96)00070-4.

788 Sayle KL, Brodie CR, Cook GT, Hamilton WD (2019) Sequential measurement of $\delta^{15}N$, $\delta^{13}C$
789     and $\delta^{34}S$ values in archaeological bone collagen at the Scottish Universities
790     Environmental Research centre (SUERC): A new analytical frontier. Rapid Commun
791     Mass Spectrom. 33:1258–1266 https://doi.org/10.1002/rcm.8462

792 Schlüchter C, Bini A, Buoncristiani JF, Coutterand S, Ellwanger D, Felber M, Florineth D,
793     Graf HR, Keller O, Kelly M, Schoeneich P (2010) Die Schweiz während des
794     letzteiszeitlichen Maximum (LGM) 1:500 000. Bundesamt für Landestopografie
795     Swisstopo, Wabern.

796 Schulze ED, Chapin FS, Gebauer G, (1994) Nitrogen nutrition and isotope differences
797     among life forms at the Northern Treeline of Alaska. Oecologia 100:406–412.
798     https://doi.org/10.1007/BF00317862.

799 Schweizer T, Schmid, E, Bay R (1959) Die «Kastelhöhle» im Kaltbrunnental, Gemeinde
800     Himmelried (Solothurn). Jahrbuch für Solothurnische Geschichte 32: 1-88.

801 Sealy, J, Johnson M, Richards MP, Nehlich O (2014) Comparison of two methods of
802     extracting bone collagen for stable carbon and nitrogen analysis: comparing whole
803     bone demineralization with gelatinization and ultrafilitration. J Archaeol Sci 47:64-69.
804     https://doi.org/10.1016/j.jas.2014.04.011.

805 Stark S (2007) Nutrient Cycling in the Tundra, in: Marschner P, Rengel Z (Eds), Nutrient
806     Cycling in Terrestrial Ecosystems, vol 10, Soil Biology, Springer, Berlin.

807 Stevens RE, Hedges REM (2004) Carbon and nitrogen stable isotope analysis of northwest
808     European horse bone and tooth collagen, 40,000 BP-present: palaeoclimatic
809     interpretations. Quaternary Sci Rev 23: 977-991.
810     https://doi.org/10.1016/j.quascirev.2003.06.024

811 Stevens RE, Jacobi R, Street M, Germonpré M, Conard NJ, Münzel SC, Hedges REM
812     (2008) Nitrogen isotope analyses of reindeer *(Rangifer tarandus)*, 45,000 BP to 9,000
813     BP: Palaeoenvironmental reconstructions. Palaeogeog Palaeocl 262:32-45.
814     https://doi.org/10.1016/j.palaeo.2008.01.019

815 Stevens RE, Hermoso-Buxán XL, Marín-Arroyo AB, González-Morales MR, Straus LG
816     (2014) Investigation of Late Pleistocene and Early Holocene palaeoenvironmental
817     change at El Mirón cave (Cantabria, Spain): insights from carbon and nitrogen isotope
818     analyses of red deer. Palaeogeogr Palaeocl 414:46-60.
819     https://doi.org/10.1016/j.palaeo.2014.05.049

820  Szpak P, Metcalfe JZ, Macdonald RA (2017) Best practices for calibrating and reporting
821      stable isotope measurements in archaeology. J Archaeol Sci Rep 13:609-
822      616. https://doi.org/10.1016/j.jasrep.2017.05.007

823  Terberger T, Street M (2002) Hiatus or continuity? New results for the question of
824      Pleniglacial settlement in Central Europe. Antiquity 76:691-698.
825      https://doi.org/10.1017/S0003598X00091134.

826  Thew N, Hadorn P, Coope R (2009) Hauterive/Rouges-Terres. Reconstruction of Upper
827      Palaeolithic and Early Mesolithic Natural Environments. Archéologie neuchâteloise,
828      44, Office et musée cantonal d'archéologie, Neuchâtel.

829  Thode HG (1991) Sulfur isotopes in nature and the environment: an overview, in: Krouse
830      HR, Grinenko VA (Eds), Stable Isotopes: Natural and Anthropogenic Sulfur in the
831      Environment, John Wiley and Sons: Chichester, pp. 1-26.

832  Trust BA, Fry B (1992) Stable sulphur isotopes in plants: a review. Plant Cell Environ
833      15:1105-10. https://doi.org/10.1111/j.1365-3040.1992.tb01661.x.

834  Vandenberghe J, French HM, Gorbunov A, Marchenko S, Velichko AA, Jin H, Cui Z, Zhang
835      T, Wan X (2014) The Last Permafrost Maximum (LPM) map of the Northern
836      Hemisphere: permafrost extent and mean annual air temperatures, 25–17 ka BP.
837      Boreas 43: 652–666. https://doi.org/110.1111/bor.12070

838  Walker RW (1957) The sulfur cycle in grassland soils. Grass Forage Sci 12:10-18.
839      https://doi.org/10.1111/j.1365-2494.1957.tb00086.x

840  Wehrli M, Tinner W, Ammann B (2007) 16,000 years of vegetation and settlement history
841      from Egelsee (Menzingen, central Switzerland). The Holocene 17(6):747-761.
842      https://doi.org/10.1177/0959683607080515

843  Weniger G-C (1989) The Magdalenian in Western Central Europe: Settlement Pattern and
844      Regionality. J World Prehist 3(3):323-372. https://doi.org/10.1007/BF00975326

845  Wißing C, Rougier H, Baumann C, Comeyne A, Crevecoeur I, Drucker DG, Gaudzinski-
846      Windheuser S, Germonpré M, Gómez-Olivencia A, Krause J, Matthies T, Naito YI,
847      Posth C, Semal P, Street M, Bocherens H. (2019) Stable isotopes reveal patterns of
848      diet and mobility in the last Neandertals and first modern humans in Europe. Sci Rep
849      9: 4433. https://doi.org/10.1038/s41598-019-41033-3.

850  Wood RE, Bronk Ramsey C, Higham TG (2010) Refining background corrections for
851      radiocarbon dating of bone collagen at ORAU. Radiocarbon 52(2): 600-611.

852

853  References appearing only in figures and tables:

854  Becker, D., Verheul, J., Zickel, M., Willmes, C. (2015): LGM paleoenvironment of Europe -
855      Map. CRC806-Database, DOI: 10.5880/SFB806.15

856   Bodu P, Debout G, Dumarçay G, Leesch D, Valentin B (2009) Révision de la chronologie
857        magdalénienne dans le Bassin parisien et alentours: nouveaux résultats, in:
858        Valentin B (Ed), Paléolithique final et Mésolithique dans le Bassin parisien et ses
859        marges. Habitats, sociétés et environnements, Projet collectif de recherche,
860        Programmes P7, P8 et P10 Rapport d'activités pour 2009, Paris, pp. 91-99.
861   Bronk Ramsey, C. (2017) Methods for Summarizing Radiocarbon Datasets. Radiocarbon
862        59(6): 1809-1833.
863   North Greenland Ice Core Project members (2004) High-resolution record of Northern
864        Hemisphere climate extending into the last interglacial period.  Nature 431(7005):
865        147-151.
866   Reimer, P. J., Bard, E., Bayliss, A., Beck, J.W., Blackwell, P.G., Ramsey, C.B., Buck, C.E.,
867        Cheng, H., Edwards, R.L., Friedrich, M., Grootes, P.M., Guilderson, T.P.,
868        Haflidason, H., Hajdas, I., Hatté, C., Heaton, T.J., Hoffmann, D.L., Hogg, A.G.,
869        Hughen, K.A., Kaiser, K.F., Kromer, B., Manning, S.W., Niu, M., Reimer, R.W.,
870        Richards, D.A., Scott, E.M., Southon, J.R., Staff, R.A., Turney, C.S.M., van der
871        Plicht, J. (2013), IntCal13 and Marine13 Radiocarbon Age Calibration Curves 0-
872        50,000 Years cal BP. Radiocarbon 55(4): 1869-1887.
873
874

| Project sample code | Species | Element | Collagen yield (%) | δ¹³C (‰) | C/N ratio | AMS Code | ¹⁴C BP | Calibrated Age BP (2σ) | Time Period | Ref |
|---|---|---|---|---|---|---|---|---|---|---|
| **Kastelhöhle-Nord, upper horizon** | | | | | | | | | | |
| UPN-232 | *Bos/Bison* | metacarpus | 10.4 | −19.5 | 3.3 | OxA-V-2794-25C | 13,550 ± 60 | 16,566–16,107 | GS-2.1a | 1 |
| | | | not given | −18.8 | not given | ETH-45024 | 13,435 ± 50 | 16,350–15,965 | GS-2.1a | 2 |
| UPN-214 | *Equus* sp. | phalanx I | 2.8 | −21.1 | 3.2 | OxA-V-2754-48C | 12,880 ± 50 | 15,605 – 15,181 | GS-2.1a | 1 |
| UPN-218 | *Equus* sp. | carpal | 8.1 | −20.4 | 3.2 | OxA-V-2748-25C | 12,560 ± 50 | 15,142 – 14,529 | GS-2.1a/GI-1e | 1 |
| UPN-212 | *Rangifer tarandus* | tibia | 5.4 | −19.6 | 3.3 | OxA-V-2793-55C | 12,380 ± 50 | 14,764 – 14,138 | GI-1ed | 1 |
| | | | not given | −18.9 | not given | ETH-45025 | 12,395 ± 45 | 14,780–14,160 | GI-1ed | 2 |
| UPN-204 | *Rangifer tarandus* | radius | 7.4 | −19.5 | 3.3 | OxA-V-2793-54C | 12,270 ± 60 | 14,740 – 14,129 | GI-1ed | 1 |
| | | | not given | −19.8 | not given | ETH-45026 | 12,215 ± 45 | 14,265–13,967 | GI-1ed | 2 |
| UPN-213 | *Rangifer tarandus* | tibia, cut-marked | 4.5 | −19.6 | 3.4 | OxA-V-2793-56C | 12,200 ± 50 | 14,260 – 13,935 | GI-1ed | 1 |
| **Monruz and Champréveyres Magdalenian** | | | | | | | | | | |
| n/a | *Equus* sp. | femur | not given | −20.3 | not given | OxA-20699 | 13,055 ± 60 | 15,874–15,349 | GS-2.1a | 3 |
| n/a | *Equus* sp. | talus | not given | −20.5 | not given | OxA-20700 | 12,815 ± 65 | 15,562–15,092 | GS-2.1a | 3 |
| n/a | *Equus* sp. | talus | not given | −20.4 | not given | OxA-20701 | 12,805 ± 75 | 15,585–15,053 | GS-2.1a | 3 |
| **Champréveyres Early Azilian** | | | | | | | | | | |
| UPN-240 | *Cervus elaphus* | metatarsal | 2.3 | −20.9 | 3.3 | OxA-V-2754-49 | 12,480 ± 50 | 15,023 – 14,284 | GS-2.1a/GI-1e | 1 |

Table 1. AMS radiocarbon determinations on bone collagen from the sites and levels discussed in the text, and as shown in Figure 2. δ¹³C and C/N ratio measured by IRMS as part of the radiocarbon dating procedure at the Oxford Radiocarbon Accelerator Unit. Calibration of radiocarbon age determinations was performed using OxCal 4.3 (Bronk Ramsey 2017) and the INTCAL13 dataset (Reimer et al. 2013). References (Ref) for dates: [1]this study; [2]Leesch and Müller, 2012; and [3]Bodu et al., 2009.

| Fauna | n | Average δ¹³C (‰) | Max δ¹³C (‰) | Min δ¹³C (‰) | Average δ¹⁵N (‰) | Max δ¹⁵N (‰) | Min δ¹⁵N (‰) | Average δ³⁴S (‰) | Max δ³⁴S (‰) | Min δ³⁴S (‰) |
|---|---|---|---|---|---|---|---|---|---|---|
| **Kastelhöhle Nord, upper horizon** | | | | | | | | | | |
| *Bos/Bison* | 6 | −19.9 ± 0.2 | −19.7 | −20.1 | 3.2 ± 0.5 | 4.0 | 2.6 | −6.1 ± 1.9 | −4.2 | −10.0 |
| *Equus sp.* | 5 | −20.8 ± 0.4 | −20.2 | −21.3 | 1.6 ± 0.5 | 2.3 | 0.7 | −2.3 ± 0.9 | −1.2 | −3.8 |
| *Rangifer tarandus* | 10 | −19.7 ± 0.3 | −19.4 | −20.3 | 2.8 ± 0.4 | 3.5 | 2.3 | −5.5 ± 1.5 | −1.3 | −7.1 |
| **Monruz** | | | | | | | | | | |
| *Equus sp.* | 7 | −21.0 ± 0.2 | −20.8 | −21.4 | 1.8 ± 0.6 | 2.9 | 1.1 | −12.3 ± 5.2 | −3.6 | −19.8 |
| *Rangifer tarandus* | 4 | −19.8 ± 0.2 | −19.6 | −20.1 | 2.8 ± 0.2 | 3.2 | 2.6 | −13.8 ± 2.9 | −10.3 | −17.3 |
| **Champréveyres** | | | | | | | | | | |
| *Cervus elaphus* | 1 | −20.7 | - | - | 2.4 | - | - | (−7.2) | - | - |

Table 2. Summary statistics for carbon, nitrogen and sulphur isotopic ratios for each species and archaeological site. Each sample was analysed in duplicated by IRMS at the Scottish Universities Environmental Research Centre. Data in () was deemed unreliable based on standard quality control criteria. Full results are presented in the Supplementary Information 1.

**Figure Captions**

876

877 Figure 1: Map showing the location of Monruz, Champréveyres and Kastelhöhle-Nord.

878 Bedrock geology is from the International Geological Map of Europe (IGME 5000; Asch

879 2005). Black line indicates present day country borders. White hatching indicates

880 reconstructed limits of Last Glacial Maximum (LGM) ice sheet extent from Becker et al.

881 (2015). Symbols indicate archaeological sites from which isotopic data used in our

882 discussion comes (full data in Supplementary Information 5), from areas that were covered

883 by ice at the LGM (pink circles) and those in areas that remained ice free throughout the

884 LGM (black squares). Inset: location of Switzerland in Europe indicated by red box.

885

886 Figure 2. Calibrated AMS radiocarbon determinations on faunal bone collagen from sites

887 discussed in the text. Calibration was performed using OxCal 4.3 (Bronk Ramsey 2017) and

888 the INTCAL13 dataset (Reimer et al. 2013) and plotted with the Last Glacial period

889 INTIMATE event stratigraphy and NGRIP ice core $\delta^{18}O$ values values (top; North Greenland

890 Ice Core Project members. 2004; Rasmussen et al., 2014). Purple = *Bos/Bison*, blue =

891 horse, red = reindeer, green = red deer. Kastelhöhle-Nord dates from this study (OxA codes)

892 and Leesch and Müller (2012; ETH codes); Monruz and Champréveyres Magdalenian dates

893 from Bodu (2009); Champréveyres Azilian dates from this study. Symbols *, ⁺, and

894 ▵ indicate date is on same bone specimen.

895

896 Figure 3.  $\delta^{13}C$, $\delta^{15}N$, and $\delta^{34}S$ values of Kastelhöhle-Nord upper horizon samples. Overlap

897 in values can be seen between *Bos/Bison* (green triangles) and reindeer (*Rangifer tarandus*,

898 orange circles), while horse (*Equus* sp., blue squares) are dissimilar in their isotopic values.

899 Enlarged symbols represent directly dated samples reported in Figure 2.
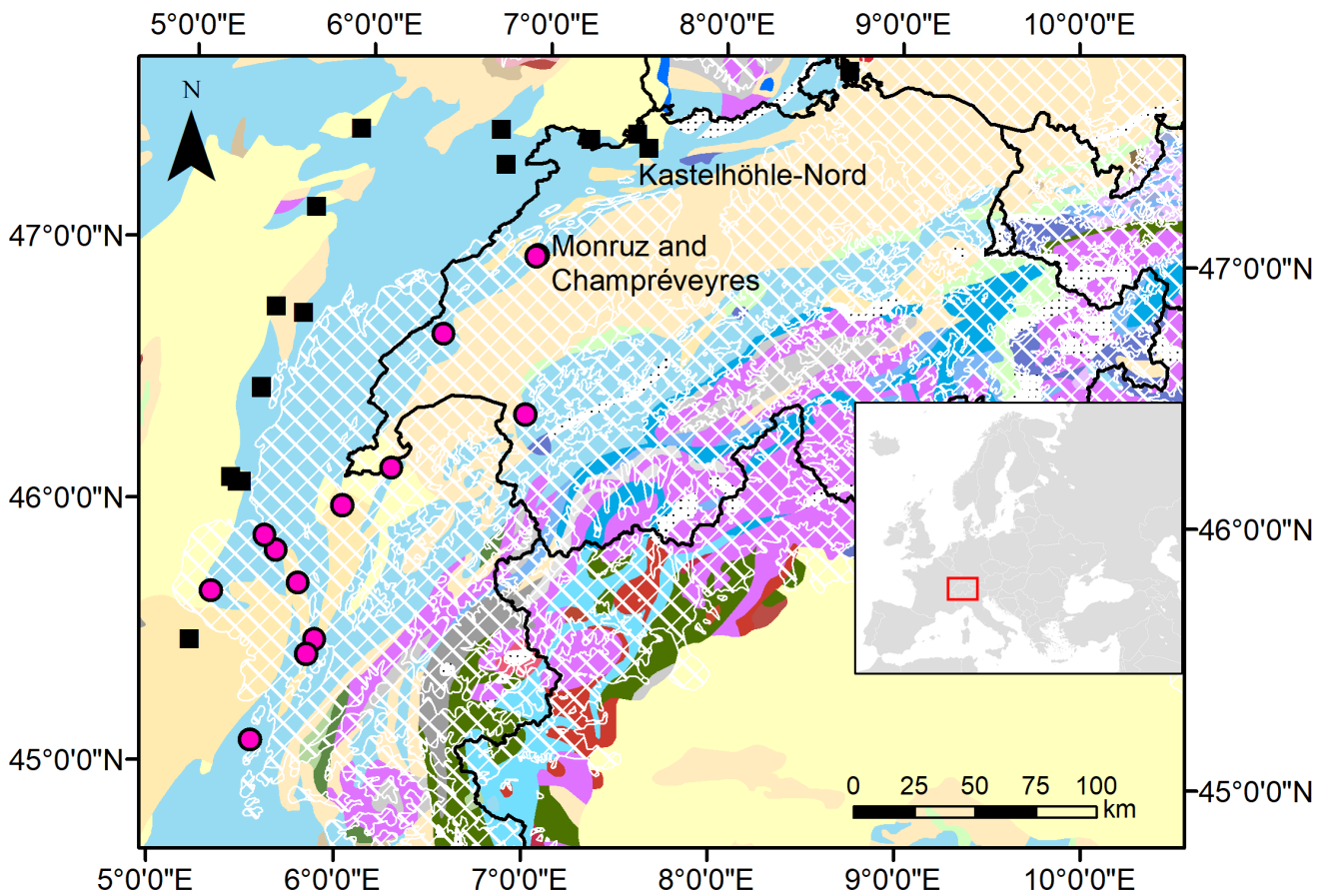
900

901 Figure 4. $\delta^{13}C$, $\delta^{15}N$, and $\delta^{34}S$ values from reindeer (*Rangifer tarandus,* circles) and horse

902 (*Equus* sp, triangles) from Kastelhöhle-Nord upper horizon (yellow) and Monruz (green).

903 $\delta^{13}C$ and $\delta^{15}N$ values cluster by species, while $\delta^{34}S$ values cluster by location.

904

905 Figure 5.  $\delta^{15}N$ (middle) and $\delta^{34}S$ (bottom) isotope values from LGM and Lateglacial fauna

906 (*Bos/Bison*, horse, red deer, reindeer) from the French and Swiss Jura, western Alps and

907 Swiss Plateau (full data in Supplementary Information 5). INTIMATE event stratigraphy and

908 NGRIP ice core $\delta^{18}O$ values (top; North Greenland Ice Core Project members. 2004;

909 Rasmussen et al., 2014). Black symbols indicate samples from locations that remained ice-

910 free throughout the LGM, pink symbols indicate samples from locations that were ice-

911    covered at the LGM, as displayed in Figure 1. Circles indicate directly dated specimens (by

912    radiocarbon), triangles indicate context dated specimens, where age has been inferred from

913    dates on other faunal specimens from the same site/stratigraphic context.
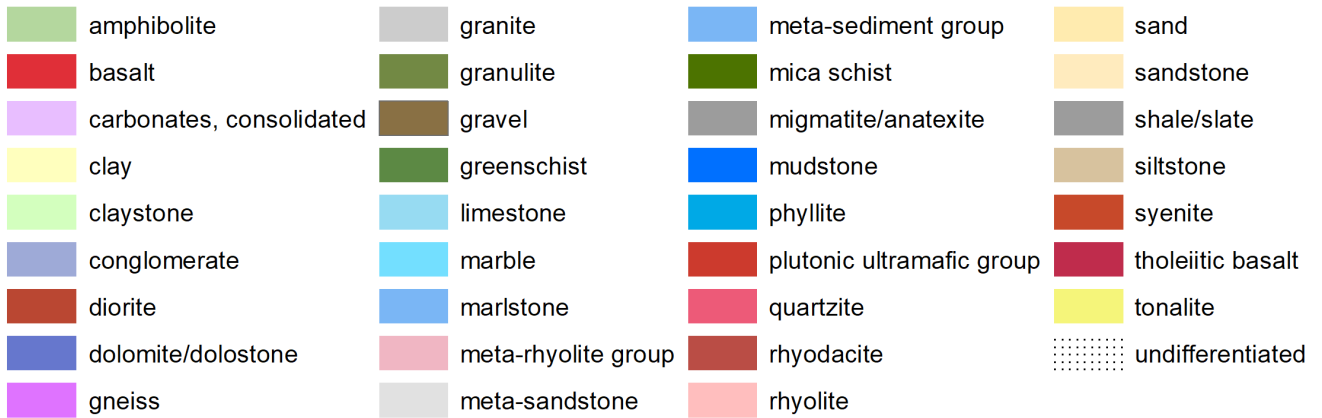
914

Figure 1

## Bedrock geology

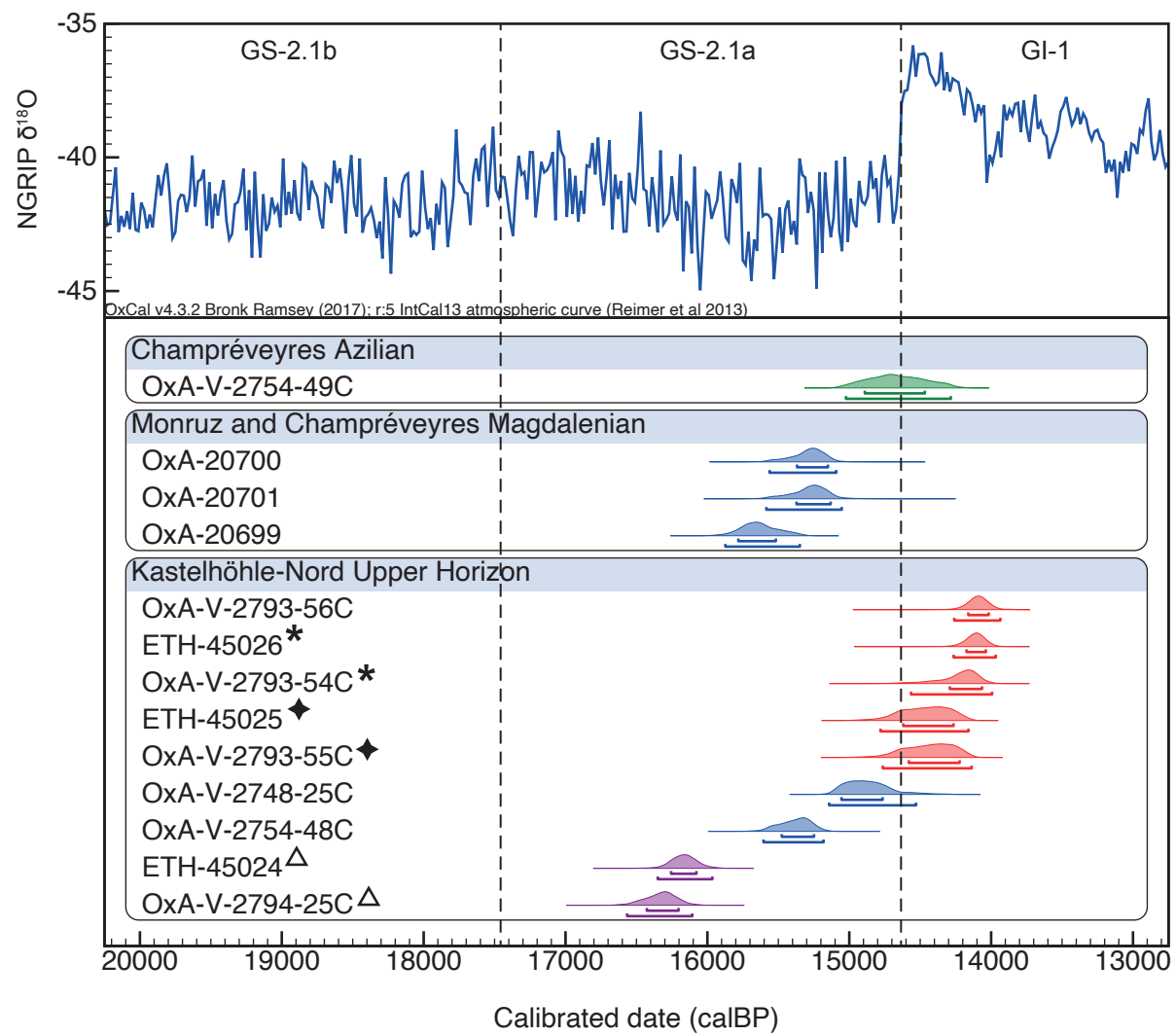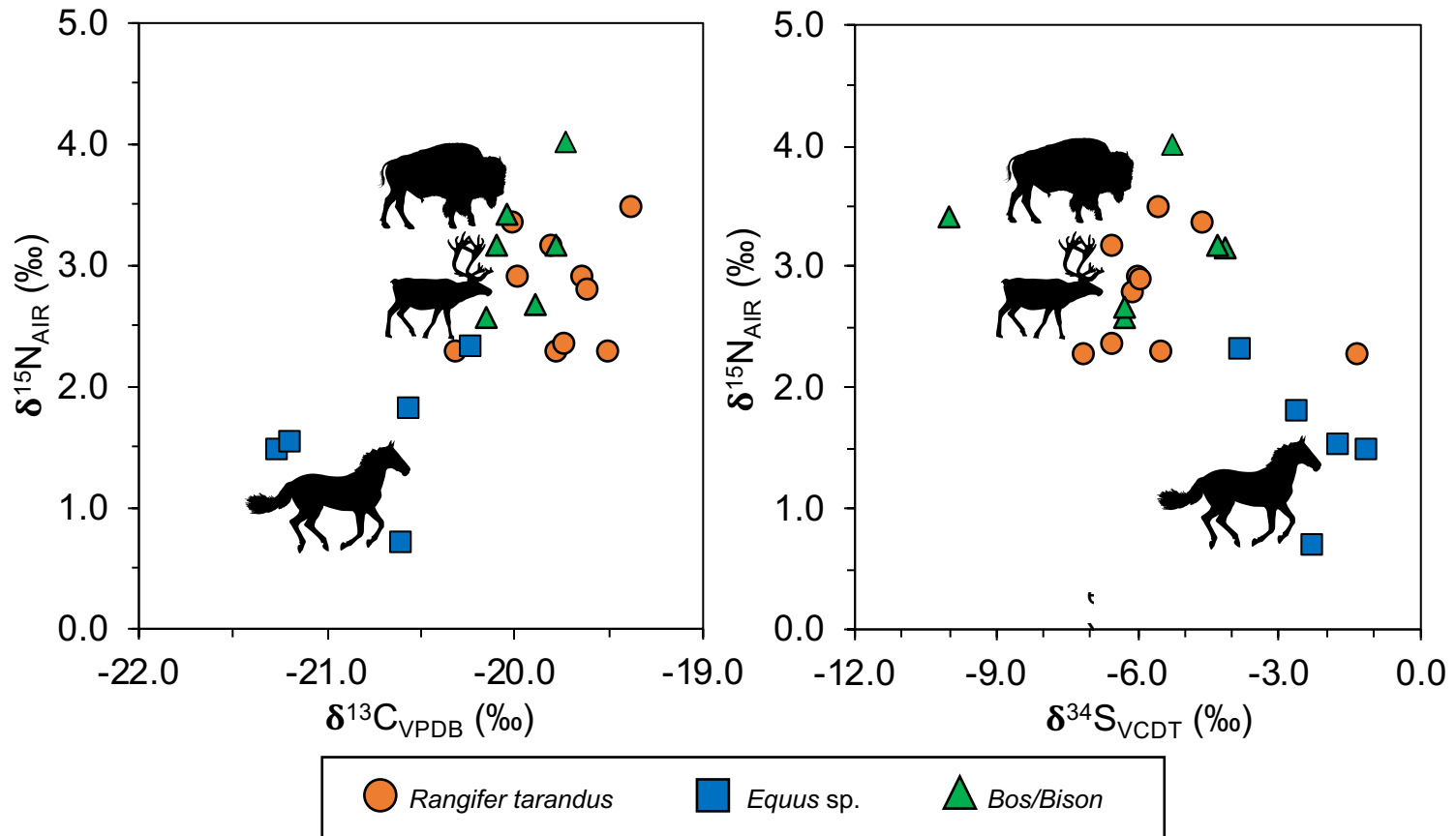| | | | |
|---|---|---|---|
| amphibolite | granite | meta-sediment group | sand |
| basalt | granulite | mica schist | sandstone |
| carbonates, consolidated | gravel | migmatite/anatexite | shale/slate |
| clay | greenschist | mudstone | siltstone |
| claystone | limestone | phyllite | syenite |
| conglomerate | marble | plutonic ultramafic group | tholeiitic basalt |
| diorite | marlstone | quartzite | tonalite |
| dolomite/dolostone | meta-rhyolite group | rhyodacite | undifferentiated |
| gneiss | meta-sandstone | rhyolite | |

Figure 2

Figure 3

Figure 4

Figure 5